One-dimensional quantum walks with single-point phase defects

Rong Zhang,[1] Peng Xue,[1,2,*] and Jason Twamley[3]

[1]*Department of Physics, Southeast University, Nanjing 211189, China*

[2]*State Key Laboratory of Precision Spectroscopy, East China Normal University, Shanghai 200062, China*

[3]*ARC Centre for Engineered Quantum Systems, Department of Physics and Astronomy, Macquarie University, North Ryde, New South Wales 2109, Australia*

(Received 3 February 2014; published 21 April 2014)

We observe the localization effect of one-dimensional quantum walks with single-point phase defects. The walker's spread velocity is dramatically suppressed by interference effects due to the phase defect. We show that the localization effect depends on four factors: the value and the position of the phase defect, the parameter of coin flipping, and the initial state of the walker + coin system.

DOI: 10.1103/PhysRevA.89.042317 PACS number(s): 03.67.Lx, 05.40.Fb, 05.45.Mt

I. INTRODUCTION

Classical random walks (RWs) have been widely used in the fields of mathematics, physics, biology, and computer science [1]. Quantum walks (QWs) are the quantum analogy of the RWs and show different properties due to interference and superposition at the quantum level compared to RWs [2]. QWs have been used to develop algorithms [3–6] which are more efficient when compared with their classical counterparts. One can use QWs to model and study biological phenomena, such as the energy transfer in photosynthesis [7], and other complex phenomenon, such as Anderson localization [8,9] and topological phases [10,11]. Furthermore, QWs are proposed to implement universal quantum computing [12–15] and perfect state transfer [16]. QWs have been realized experimentally in NMR systems [17–19], trapped ions [20,21], trapped neutral atoms [22,23] and photons in beam splitter arrays [24–26], fibers [27–30], and laser-writing waveguides [31–33].

Since QWs have been used widely as mentioned above, it is necessary to study the properties of QWs in detail. The impact of the decoherence on the QWs [34–37] has been studied and under the influence of decoherence QWs are transformed to RWs with a loss of quantum coherence [38,39]. Static disorder alters QWs' ballistic spread to localization through a disruption of the interference pattern [40–43], while RWs with disorder can still move infinitely slowly [44]. In this paper, we focus on the impact of a single-point phase defect (SPPD) on the 1D coined QW on a line whose properties are usually described by the walker's position distribution and variance. We find that for 1D QWs with an SPPD the walker's spread can be greatly suppressed by choosing the proper point defect and initial state of the walker + coin system indicating a type of localization effect. Such nonclassical properties of 1D QWs with SPPD show some similarity to quantum resonances in quantum chaos and may be useful to model and study quantum chaos. They may also be useful to simulate trapped localized excitations, e.g., defect scattering in condensed matter systems.

*gnep.eux@gmail.com

II. SPREAD SUPPRESSION OF A 1D QW WITH SPPD

A standard 1D QW (without SPPD) consists of a coin and a walker. The total Hilbert space of the walker + coin system $\mathcal{H}_c \otimes \mathcal{H}_w$ is spanned by $|c=0,1\rangle$ and $|x\rangle$ ($x \in \mathbb{Z}$ and x is the position of the walker along the x axis). One-step evolution of the system involves the coin flipping and conditional position shift based on the outcome of the coin flipping. The corresponding unitary operation U is

$$U = \left(\sum_{c=0,1} |c\rangle\langle c| \otimes S_c\right)[C \otimes I], \tag{1}$$

where

$$C = \frac{1}{\sqrt{2}}\begin{pmatrix} 1 & 1 \\ 1 & -1 \end{pmatrix} \tag{2}$$

is the coin flipping operator, i.e., Hadamard operation. The conditional position shift operator S_c takes the form $S_c|x\rangle = |x+(-1)^c\rangle$. Without loss of generality, we assume the walker is at the position $x=0$ initially, and the initial coin state is the superposition of $|0\rangle$ and $|1\rangle$. Thus the initial state of the whole system is $|\psi(0)\rangle = (a|0\rangle + b|1\rangle)_c \otimes |0\rangle_w$ with $|a|^2 + |b|^2 = 1$. The final state of the system after t steps evolution is $|\psi(t)\rangle = U^t|\psi(0)\rangle$. We show the properties of the 1D QW with SPPD via position distribution P_w and the position variance $\sigma^2 = \langle x^2\rangle - \langle x\rangle^2$. The walker positions after evolution can be calculated through the partial trace on the coin of the final state $|\psi(t)\rangle$.

We study the impact of SPPD on 1D QW in this paper. The single-point phase shift $\phi \in (0,2\pi]$ is applied whenever the walker passes through a preset position $x=n$. In this case, the unitary operation U_ϕ can be expressed as

$$U_\phi = \left(\sum_{c=0,1} |c\rangle\langle c| \otimes S_c(\phi)\right)[C \otimes I], \tag{3}$$

where $S_c(\phi)|x\rangle = e^{i\phi\delta_{x,n}}|x+(-1)^c\rangle$; we note that the defect phase is accrued irrespective of the coin state, i.e., direction of the walker. The properties of a 1D QW with SPPD will be discussed below and following that we will give various explanations for their behavior.

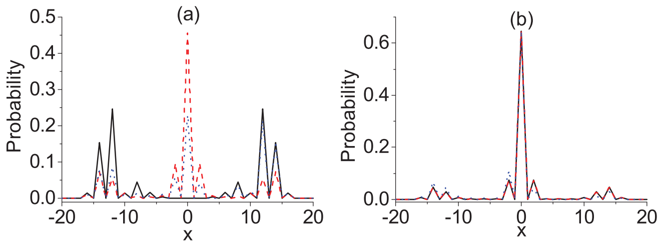

FIG. 1. (Color online) Probability distributions of the 1D QWs with an SPPD ϕ located at the original position of the QW for different initial coin states. (a) $\phi = \pi/4$, (b) $\phi = \pi$. The solid black lines correspond to $|\psi_s\rangle_c$, the dashed red lines correspond to $|\psi_a\rangle_c$, and the dotted blue lines correspond to $|\psi_{as}\rangle_c$.

A. 1D QW with SPPD at the origin of the walker

First, we apply the SPPD ϕ to be co-located at $x = 0$ of the 1D QW and compare the subsequent position probability distributions to the standard Hadamard QW (without SPPD). The probability distributions after 20 steps with the initial symmetric $|\psi_s\rangle_c = (|0\rangle + i|1\rangle)/\sqrt{2}$, antisymmetric $|\psi_a\rangle_c = (|0\rangle - i|1\rangle)/\sqrt{2}$, and asymmetric coin states $|\psi_{as}\rangle_c = |0\rangle$ and the SPPD $\phi = \pi/4$ or $\phi = \pi$ at $x = 0$ are shown in Fig. 1(a) and Fig. 1(b), respectively. With SPPD $\phi = \pi/4$ at $x = 0$, we observe that for the antisymmetric initial coin state, the evolution is localized at the origin ($x = 0$). After twenty steps the $P_w(x = 0, t = 20) \approx 0.45$, while for the symmetric and asymmetric initial coin states $|\psi_s\rangle_c$, $|\psi_{as}\rangle_c$ no localization effect is observed. However, if the SPPD ϕ at $x = 0$ is increased to π, localization at the origin $x = 0$ can be observed for all three initial coin states, and $P_w(0,20) \approx 0.65$.

Thus the localization effect of 1D QWs with SPPD at the origin of the QW depends both on the initial coin state and the value of SPPD ϕ as shown in Fig. 1. To obtain a more quantitative gauge of the degree of localization, the ratio of variances $\sigma^2(\phi)/\sigma^2(\phi = 0)$ of 1D QW with SPPD ϕ in $x = 0$ is shown in Fig. 2. The variance of the 1D QW with SPPD ϕ at $x = 0$ is bigger than that of RW, and we observe a type of "repulsive" behavior when $|\psi_s\rangle_c$ and $\phi = \pi/4$ with the defect QW expanding faster than the standard Hadamard QW. However, the variance of other cases is less than that of the standard QW. Numerical simulations indicate that this "repulsive" expansion can be enhanced for SPPD $\phi < \pi/2$ located at the position $x = 0$ with the initial state $|\psi_s\rangle_c$.

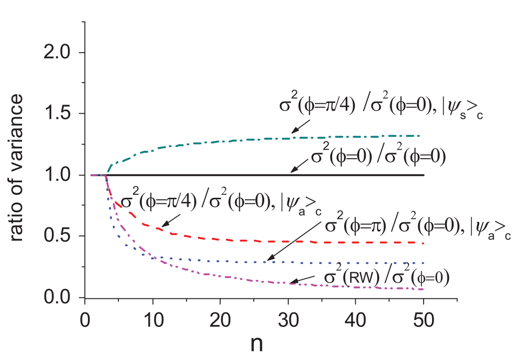

FIG. 2. (Color online) Plot of ratio of variance $\sigma^2(\phi)/\sigma^2(\phi = 0)$ of 1D QWs with the different value ϕ of SPPD at origin and different initial coin states as a function of n, number of steps.

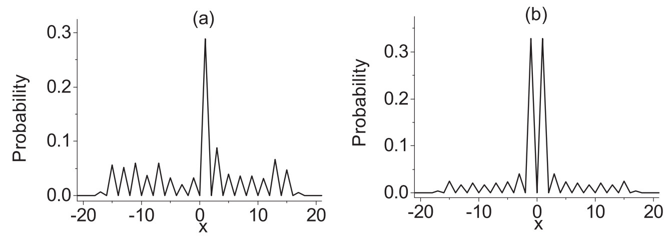

FIG. 3. (a) The distribution of the 1D QW with SPPD $\phi = \pi/2$ at $x = 1$, the initial coin state $|\psi_a\rangle_c$ after 21 steps. (b) The distribution of the 1D QW with SPPD $\phi = \pi/2$ at both $x = 1$ and $x = -1$ with $|\psi_a\rangle_c$ after 21 steps.

B. 1D QW with SPPD in an arbitrary position $x = n$ ($n \neq 0$)

We have studied in detail the properties of a 1D QW with an SPPD ϕ at the origin of the QW. Let us now consider SPPD ϕ at the position $x = n$ ($n \neq 0$) which is not at the origin location of the QW. With SPPD $\phi = \pi/2$ in $x = 1$, the initial coin state $|\psi_a\rangle_c$, the walker is nearly trapped in the position $x = 1$ with $P_w(x = 1) \approx 0.3$ after 21 steps as shown in Fig. 3(a) and numerical simulations show that the walker has the maximal occupation at $x = 1$ with an odd step for an SPPD in the range $\phi \in (\pi/4, \pi]$. When an SPPD $\phi = \pi/2$ is added at $x = -1$, localization in the position $x = -1$ after an odd step can also be observed. The distributions with SPPD $x = -1$ behave similarly to those at $x = 1$. However, numerically we observe that no localization is possible in 1D QW with the SPPD located at positions $x \geqslant 2$ for any initial state of the coin.

When SPPDs $\phi = \pi/2$ are added at both $x = 1$ and $x = -1$, with the initial coin state $|\psi_a\rangle_c$, the walker localizes at $x = 1$ and $x = -1$ with high probabilities $P_w(x = 1) = P_w(x = -1) \approx 0.3$ after odd steps (21 steps) as shown in Fig. 3(b).

III. DISCUSSION

We now seek to explain the localization effect [45] of 1D QW with SPPD. The eigenstates $|\varphi\rangle$ of the unitary operation of 1D QW with SPPD, U_ϕ^2, can be found analytically. If the initial state of the walker + coin system is in such an eigenstate, then under the evolution by application of U_ϕ, it remains in a stationary state. The profiles of stationary eigenstates can be obtained by tracing out the coin state as shown in the following subsection.

In the normal QW without an SPPD the eigenstates $|\varphi_k\rangle$, which for a finite domain are discrete, are completely delocalised over the position Hilbert space of the walker. We will discover below that with the introduction of an SPPD, highly localized stationary states $|\widetilde{\varphi}_k\rangle$ appear within the spectrum of eigenstates $\{|\varphi\rangle_k\}$. We find that when the initial state has large support on the localized eigenstate, i.e. $F = \sum_k |\langle\widetilde{\varphi}_k|\psi(t = 0)\rangle|^2$, the time evolved state will display strong localization effects and F will stay large.

Numerical calculations show that there are no localized eigenstates for U^2 in Eq. (1) for the 1D standard Hadamard QWs (without SPPD). Thus the standard QW does not exhibit localization. For QW with SPPD at the position $x = n$, the eigenstates for U_ϕ^2 depend on the value ϕ and the position n of the SPPD, with the appropriate choices of ϕ some of the eigenstates exhibit localization. Thus by choosing the proper initial wave-function so that $1 \geqslant F \gg 0$, large localization can be observed for 1D QWs with SPPDs.

A. Localized eigenstates of the unitary operation for 1D QW with SPPD

We now analytically explore the eigenstate structures of the unitary operation U_ϕ^2 for the 1D QW with SPPD. The state of the whole system is described as:

$$|\Psi\rangle = \sum_x (a_x|0\rangle_c|x\rangle_w + b_x|1\rangle_c|x\rangle_w). \tag{4}$$

According to the evolution under U_ϕ^2, the walker acquires SPPD $w = e^{i\phi}$ with $\phi \in (0,2\pi]$ when the walker is at even position $x = 2n$, thus the amplitudes corresponding to the walker at position $x = 2n$ satisfy:

$$\begin{aligned} \sqrt{2}a_{2n-1}(t+1) &= wa_{2n}(t) + wb_{2n}(t),\\ \sqrt{2}b_{2n+1}(t+1) &= wa_{2n}(t) - wb_{2n}(t), \end{aligned} \tag{5}$$

and the amplitudes corresponding to the walker at the other positions $x \neq 2n$ satisfy:

$$\begin{aligned} \sqrt{2}a_x(t+1) &= a_{x+1}(t) + b_{x+1}(t),\\ \sqrt{2}a_x(t+1) &= a_{x-1}(t) - b_{x-1}(t). \end{aligned} \tag{6}$$

It is convenient to consider the double step operator U_ϕ^2 since the walker's position after even steps does not interfere with those after odd steps, the amplitudes of the eigenstates take the time-independent form:

$$2\lambda\bar{a}_n = \bar{a}_{n+1} + \bar{b}_{n+1} + w\bar{a}_n - w\bar{b}_n, \tag{7}$$

$$2\lambda\bar{b}_n = w\bar{a}_n + w\bar{b}_n - \bar{a}_{n-1} + \bar{b}_{n-1}, \tag{8}$$

$$2\lambda\bar{a}_{n-1} = w\bar{a}_n + w\bar{b}_n + \bar{a}_{n-1} - \bar{b}_{n-1}, \tag{9}$$

$$2\lambda\bar{b}_{n+1} = \bar{a}_{n+1} + \bar{b}_{n+1} - w\bar{a}_n + w\bar{b}_n, \tag{10}$$

and

$$2\lambda\bar{a}_x = \bar{a}_{x+1} + \bar{b}_{x+1} + \bar{a}_x - \bar{b}_x, \quad x \neq n,n-1, \tag{11}$$

$$2\lambda\bar{b}_x = \bar{a}_x + \bar{b}_x - \bar{a}_{x-1} + \bar{b}_{x-1}, \quad x \neq n,n+1, \tag{12}$$

where λ is the eigenvalue of U_ϕ^2. We assume $\bar{a}_x = a_{2x}, \bar{b}_x = b_{2x}$ for convenience. From Eqs. (11) and (12), we can obtain

$$\bar{b}_{x+1} = (\bar{a}_{x+1} - \lambda\bar{a}_x)/(\lambda - 1), \quad x \neq n-1,n \tag{13}$$

by using Eq. (13) together with Eqs. (11) and (12), we get:

$$\lambda\bar{a}_{x+1} - 2(\lambda^2 - \lambda + 1)\bar{a}_x + \lambda\bar{a}_{x-1} = 0. \tag{14}$$

The general solution of the above equation is $\bar{a}_x = c_1 y^x + c_2 y^{-x}$. Here y satisfies the equation

$$\lambda y^2 - 2(\lambda^2 - \lambda + 1)y + \lambda = 0; \tag{15}$$

so does $1/y$. For $x \to \pm\infty$, the amplitude of the wave-function must have $\bar{a}_x \to 0$ due to normalization, therefore

$$\begin{aligned} \bar{a}_x &= c_1 y^x, \quad x \geqslant n+1,\\ \bar{a}_x &= c_2 y^{-x}, \quad x \leqslant n-1. \end{aligned} \tag{16}$$

Thus

$$\begin{aligned} \bar{b}_x &= c_1 \frac{y-\lambda}{\lambda - 1} y^{x-1}, \quad x \geqslant n+1.\\ \bar{b}_x &= c_2 \frac{1-\lambda x}{\lambda - 1} y^{-x}, \quad x \leqslant n-1. \end{aligned} \tag{17}$$

From Eqs. (7) and (10) we can get

$$\bar{a}_n = 1/\lambda[\bar{a}_{n+1} + \bar{b}_{n+1}(1-\lambda)]. \tag{18}$$

Substitute Eqs. (16) and (17) into Eqs. (18) and we get

$$\bar{a}_n = c_1. \tag{19}$$

From Eqs. (8) and (9) we find

$$\bar{b}_n = [\bar{b}_{n-1} + \bar{a}_{n-1}(\lambda - 1)]/\lambda. \tag{20}$$

Thus from Eqs. (15)–(17) we can obtain

$$\bar{b}_n = c_2 \frac{1-\lambda y}{\lambda - 1}. \tag{21}$$

From Eqs. (16) and (17) and Eqs. (7) and (8) we have

$$\begin{aligned} w\bar{b}_n &= c_1\left(y + w - 2\lambda + \frac{y-\lambda}{\lambda-1}\right),\\ c_1 w &= \bar{b}_n\left(2\lambda - y - w + y\frac{\lambda - 1}{1-\lambda y}\right). \end{aligned} \tag{22}$$

The above equation together with Eq. (15) we can show:

$$y_\pm = \frac{1}{2\cos(\phi) \mp 2\sin(\phi) - 3}. \tag{23}$$

From Eqs. (21)–(23) we find $c_2^\pm = c_1^\pm(w \mp iw \pm i)$. Therefore we can get the amplitude of the localized stationary state as

$$\bar{a}_n^{(\pm)} = c_1^\pm, \quad \bar{b}_n^{(\pm)} = \mp i c_1^\pm \tag{24}$$

and

$$\begin{aligned} \bar{a}_x^{(\pm)} &= c_1^\pm y_\pm^x, \quad x \geqslant n+1,\\ \bar{a}_x^{(\pm)} &= c_1^\pm(w \mp iw \pm i)y_\pm^{-x}, \quad x \leqslant n-1,\\ \bar{b}_x^{(\pm)} &= c_1^\pm(1 - w \mp iw)y_\pm^x, \quad x \geqslant n+1,\\ \bar{b}_x^{(\pm)} &= \mp i c_1^\pm y_\pm^{-x}, \quad x \leqslant n-1, \end{aligned} \tag{25}$$

with $c_1^\pm = \sqrt{\frac{1+y_\pm}{2}}$. We have explored the eigenstate structure of 1D QW with an SPPD at even position $x = 2n$ analytically and we can analyze the localized eigenstate structure similarly when the walker acquires an SPPD at odd position $x = 2n+1$.

We consider the case of QW with an SPPD at origin. The probability distributions of all eigenstates of the unitary operation U_ϕ^2 with $\phi = \pi/4$ and $\phi = \pi$ are shown in Fig. 4. We observe one localized eigenstate when $\phi = \pi/4$ [Fig. 4(b)], but when the SPPD $\phi = \pi$, there are two degenerated localized eigenstates exhibiting the same profile [Fig. 4(d)]. In Figs. 4(b) and 4(d), the comparison between the analytic results (in black

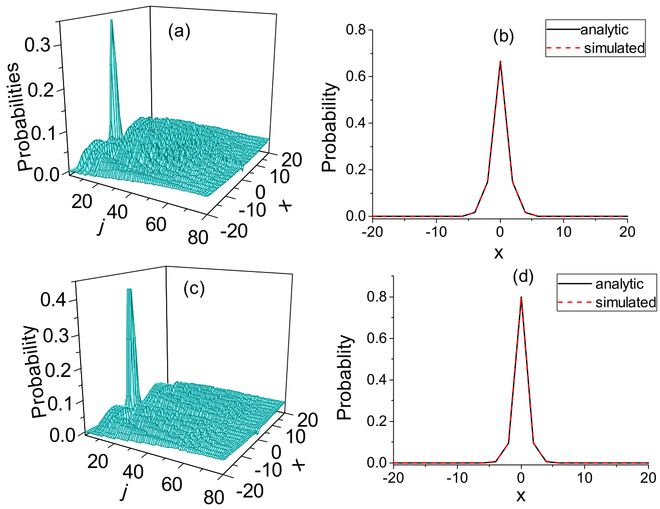

FIG. 4. (Color online) The profiles of all eigenstates of U_ϕ^2 for 1D QW with different value of SPPD in the position $x = 0$ (a) $\phi = \pi/4$ and (c) $\phi = \pi$ where j labels the eigenstate and we have truncated to 41 spatial lattice sites. The corresponding localized eigenstates are shown in (b) and (d), respectively.

lines) via Eqs. (24), (25), etc., and the simulation results (in red lines) is perfect.

Next we analyze the case of 1D QW with SPPD in the certain position $x = n$ ($n \neq 0$). Numerical calculations show that there are several eigenstates exhibiting localization in the position $x = n (n \neq 0)$. For example, the profiles of eigenstates of U_ϕ for 1D QW with SPPD $\phi = \pi/2$ in the position $x = 1$ are shown in Fig. 5. The profiles of all eigenstates with SPPD $\phi = \pi/2$ are shown in Fig. 5(a). For 1D QW with SPPD $\phi = \pi/2$ in the position $x = 1$, there is one localized eigenstate of U_ϕ^2 and exhibit the same profile as shown in Fig. 5(b).

B. Overlap between the initial state of 1D QW with SPPD and the localized eigenstates

We have shown the profiles of the eigenstates of the unitary operation for 1D QW with SPPD and some of the eigenstates exhibit localization due to SPPD breaking the interference pattern. We now study the overlap F between the chosen initial state and localized eigenstates of U_ϕ. The analytical result of

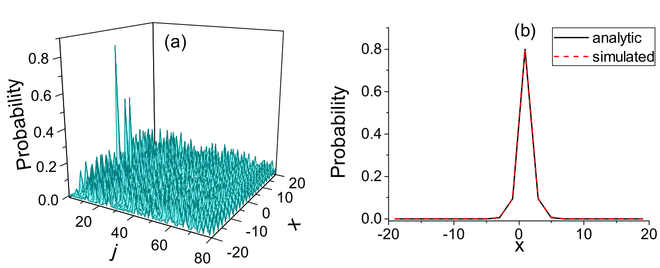

FIG. 5. (Color online) The plots of the profiles of all eigenstates of U_ϕ^2 for 1D QW with the SPPD $\phi = \pi/2$ at $x = 1$ are shown in (a). The corresponding nondegenerate localized eigenstates are shown in (b).

overlap for the symmetric initial state $|\psi_s\rangle_c$ is

$$F_1 = 1/2(|\bar{a}_0^+|^2 - i\bar{b}_0^+\bar{a}_0^{+*} + i\bar{a}_0^+\bar{b}_0^{+*} + |\bar{b}_0^{+*}|^2) + |\bar{a}_0^-|^2 - i\bar{b}_0^-\bar{a}_0^{-*} + i\bar{a}_0^-\bar{b}_0^{-*} + |\bar{b}_0^{-*}|^2), \quad (26)$$

for antisymmetric initial state $|\psi_a\rangle_c$, the overlap is

$$F_2 = 1/2(|\bar{a}_0^+|^2 + i\bar{b}_0^+\bar{a}_0^{+*} - i\bar{a}_0^+\bar{b}_0^{+*} + |\bar{b}_0^{+*}|^2) + |\bar{a}_0^-|^2 + i\bar{b}_0^-\bar{a}_0^{-*} - i\bar{a}_0^-\bar{b}_0^{-*} + |\bar{b}_0^{-*}|^2), \quad (27)$$

while for asymmetric initial state $|\psi_{as}\rangle_c$

$$F_3 = |\bar{a}_0^+|^2 + |\bar{a}_0^-|^2, \quad (28)$$

where $\bar{a}_0$ and $\bar{b}_0$ are the amplitude of the coin state $|0\rangle$ and $|1\rangle$ when the walker is at $x = 0$ and can be obtained from Eqs. (23)–(25) with normalization condition. From Eqs. (26)–(28), the overlap depends on the initial state, the position of the SPPD, and the value of the SPPD ϕ. When the overlap $1 \geqslant F \gg 0$, the 1D QWs with SPPD and the chosen initial state show the localization effect.

We consider 1D QW with SPPD in the original position $x = 0$ first. The overlap F depends on the value ϕ of SPPD and the initial state as shown in Fig. 6. The figure shows F as a function of the value of ϕ for 1D QW with Hadamard coin flipping and three different initial states. For $|\psi(t = 0)\rangle = |\psi\rangle_c \otimes |0\rangle_w$ with $|\psi_c\rangle = |\psi_a\rangle_c$ the overlap satisfies $1 \geqslant F \gg 0$ for $\phi \in (0, 3\pi/2]$, and the state is localized, whereas for $|\psi_s\rangle_c$, $1 \geqslant F \gg 0$ for $\phi \in (\pi/2, 2\pi]$, and thus localization is observed only in the restricted range. For $|\psi_{as}\rangle_c$, $1 \geqslant F \gg 0$ for $\phi \in (\pi/4, 7\pi/4)$. From this we can better understand why the localization depends on the value of the SPPD ϕ and the initial coin state.

We can also use the overlap to explain the localization effect of 1D QW which starts at the origin $x = 0$ and whereas SPPD localized at $x = n$ ($n \neq 0$). The initial overlap F depends on the spatial separation between the origin of the QW and position n of SPPD (see Fig. 7). The overlap F decreases nearly to 0 for $n \geqslant 2$. Thus we can now see why localization cannot be observed in 1D QW with an SPPD at $x = n$ ($n \geqslant 2$) though

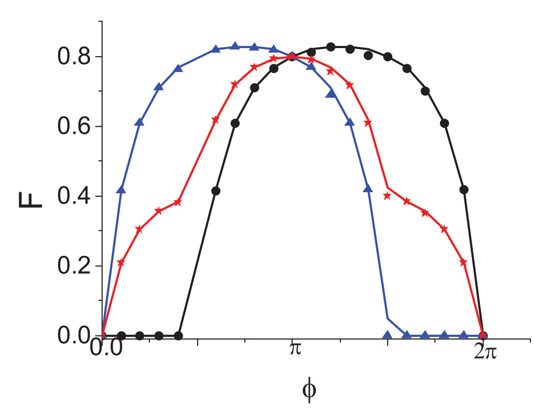

FIG. 6. (Color online) The overlaps F between the initial states and localized eigenstates as a function of the value of SPPD ϕ. The solid lines correspond to analytical results and the dotted lines correspond to the simulated results. The black line and circle dot correspond to the initial coin state $|\psi_s\rangle_c$, the blue line and triangle dot correspond to the initial coin state $|\psi_a\rangle_c$, and the red line and pentagonal dot correspond to the initial coin state $|\psi_{as}\rangle_c$.

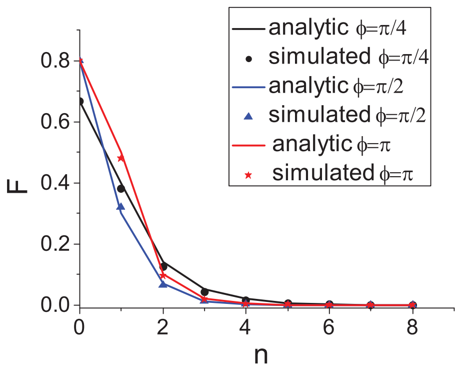

FIG. 7. (Color online) The overlap F between the asymmetric initial state $|\psi_a\rangle_c$ and the localized eigenstates of U as a function of the position n of SPPD with the value of the SPPD $\phi = \pi/4$ (black line and circle dot), $\phi = \pi/2$ (blue line and triangle dot), and $\phi = \pi$ (red line and pentagonal dot). Solid lines correspond to the analytical results and dot lines correspond to the simulated results.

there are localized stationary states. However a localization effect for 1D QW with SPPD at the position $x = 1$ can be observed as shown in Fig. 3(a).

IV. CONCLUSIONS

In conclusion, we have shown the nonclassical properties of the 1D QW with SPPD. The walker's spread velocity can be either enhanced or diminished compared to the standard QWs by adding an SPPD and this also depends on the coin initial state. We can understand the localization effect in 1D localized QWs by studying the eigenstates of the unitary walk evolution operation and the overlap of the walker's initial state with the localized eigenstates. The interesting superexpansion and suppression of the walker's spread velocity may be useful to build new quantum algorithms and simulations.

ACKNOWLEDGMENTS

This work has been supported by the National Natural Science Foundation of China under Grants No. 11004029 and No. 11174052, the Natural Science Foundation of Jiangsu Province under Grant No. BK2010422, the Ph.D. program of the Ministry of Education of China, the Excellent Young Teachers Program of Southeast University, the Open Fund from the SKLPS of ECNU, and the National Basic Research Development Program of China (973 Program) under Grant No. 2011CB921203. We acknowledge funds from the ARC Center of Excellence in Engineered Quantum Systems (CE110001013).

[1] N. Guillotin-Plantard and R. Schott, *Dynamic Random Walks: Theory and Application* (Elsevier, Amsterdam, 2006).
[2] Y. Aharonov, L. Davidovich, and N. Zagury, Phys. Rev. A **48**, 1687 (1993).
[3] A. Ambainis, Int. J. Quantum Inf. **1**, 507 (2003).
[4] A. M. Childs *et al.*, *Proceedings of the 35th ACM Symposium on Theory of Computing (STOC)* (ACM Press, New York, 2003), pp. 59–68.
[5] N. Shenvi, J. Kempe, and K. B. Whaley, Phys. Rev. A **67**, 052307 (2003).
[6] J. Kempe, Contemp. Phys. **44**, 307 (2003).
[7] A. C. Oliveira, R. Portugal, and R. Donangelo, Phys. Rev. A **74**, 012312 (2006).
[8] T. A. Brun, H. A. Carteret, and A. Ambainis, Phys. Rev. Lett. **91**, 130602 (2003).
[9] A. Crespi, R. Osellame, R. Ramponi, V. Giovannetti, R. Fazio, L. Sansoni, F. D. Nicol, F. Sciarrino, and P. Mataloni, Nat. Photonics **7**, 322 (2013).
[10] T. Kitagawa, M. S. Rudner, E. Berg, and E. Demler, Phys. Rev. A **82**, 033429 (2010).
[11] T. Kitagawa, M. A. Broome, A. Fedrizzi, M. S. Rudner, E. Berg, I. Kassal, A. Aspuru-Guzik, E. Demler, and A. G. White, Nat. Commun. **3**, 882 (2012).
[12] A. M. Childs, Phys. Rev. Lett. **102**, 180501 (2009).
[13] A. M. Childs, D. Gosset, and Z. Webb, Science **339**, 791 (2013).
[14] N. B. Lovett, S. Cooper, M. Everitt, M. Trevers, and V. Kendon, Phys. Re. A **81**, 042330 (2010).
[15] V. Kendon and O. Maloyer, Theor. Comput. Sci. **394**, 187 (2007).
[16] P. Kurzyński and A. Wójcik, Phys. Rev. A **83**, 062315 (2011).
[17] J. Du, H. Li, X. Xu, M. Shi, J. Wu, X. Zhou, and R. Han, Phys. Rev. A **67**, 042316 (2003).
[18] C. A. Ryan, M. Laforest, J. C. Boileau, and R. Laflamme, Phys. Rev. A **72**, 062317 (2005).
[19] D. Lu, J. Zhu, P. Zou, X. Peng, Y. Yu, S. Zhang, Q. Chen, and J. Du, Phys. Rev. A **81**, 022308 (2010).
[20] F. Zähringer, G. Kirchmair, R. Gerritsma, E. Solano, R. Blatt, and C. F. Roos, Phys. Rev. Lett. **104**, 100503 (2010).
[21] H. Schmitz, R. Matjeschk, Ch. Schneider, J. Glueckert, M. Enderlein, T. Huber, and T. Schaetz, Phys. Rev. Lett. **103**, 090504 (2009).
[22] R. Cote, A. Russell, E. E. Eyler, and P. L. Gould, New J. Phys. **8**, 156 (2006).
[23] M. Karski, L. Förster, J. Choi, A. Steffen, W. Alt, D. Meschede, and A. Widera, Science **325**, 174 (2009).
[24] B. Do, M. L. Stohler, S. Balasubramanian, D. S. Elliott, C. Eash, E. Fischbach, M. A. Fischbach, A. Mills, and B. Zwickl, J. Opt. Soc. Am. B **22**, 499 (2005).
[25] M. A. Broome, A. Fedrizzi, B. P. Lanyon, I. Kassal, A. Aspuru-Guzik, and A. G. White, Phys. Rev. Lett. **104**, 153602 (2010).
[26] T. Kitagawa, M. A. Broome, A. Fedrizzi, M. S. Rudner, E. Berg, I. Kassal, A. Aspuru-Guzik, E. Demler, and A. G. White, Nat. Commun. **3**, 882 (2012).
[27] A. Schreiber, K. N. Cassemiro, V. Potoček, A. Gábris, P. J. Mosley, E. Andersson, I. Jex, and Ch. Silberhorn, Phys. Rev. Lett. **104**, 050502 (2010).
[28] A. Schreiber1, K. N. Cassemiro, V. Potoček, A. Gábris, I. Jex, and Ch. Silberhorn, Phys. Rev. Lett. **106**, 180403 (2011).

[29] A. Peruzzo, M. Lobino, J. C. F. Matthews, N. Matsuda, A. Politi, K. Poulios, X. Zhou, Y. Lahini, N. Ismail, K. Wörhoff, Y. Bromberg, Y. Silberberg, M. G. Thompson, and J. L. OBrien, Science **329**, 1500 (2010).
[30] A. Schreiber, A. Gbris, P. P. Rohde, K. Laiho, M. Štefak, V. Potoček, C. Hamilton, I. Jex, and Ch. Silberhorn, Science **336**, 55 (2012).
[31] A. Crespi, R. Osellame, R. Ramponi, V. Giovannetti, R. Fazio, L. Sansoni, F. D. Nicola, F. Sciarrino, and P. Mataloni, Nat. Photonics **7**, 322 (2013).
[32] J. O. Owens, M. A. Broome, D. N. Biggerstaff, M. E. Goggin, A. Fedrizzi, T. Linjordet, M. Ams, G. D. Marshall, J. Twamley, M. J. Withford, and A. G. White, New J. Phys. **13**, 075003 (2011).
[33] L. Sansoni, F. Sciarrino, G. Vallone, P. Mataloni, A. Crespi, R. Ramponi, and R. Osellame, Phys. Rev. Lett. **108**, 010502 (2012).
[34] P. Xue and B. C. Sanders, New J. Phys. **10**, 053025 (2008).
[35] P. Xue, B. C. Sanders, and D. Leibfried, Phys. Rev. Lett. **103**, 183602 (2009).
[36] V. Kendon and B. Tregenna, Phys. Rev. A **67**, 042315 (2003).
[37] V. Kendon and B. Tregenna, Lect. Notes Phys. **633**, 253 (2004).
[38] P. Xue, B. C. Sanders, A. Blais, and K. Lalumiére, Phys. Rev. A **78**, 042334 (2008).
[39] A. Schreiber, K. N. Cassemiro, V. Potoček, A. Gábris, I. Jex, and Ch. Silberhorn, Phys. Rev. Lett. **106**, 180403 (2011).
[40] A. Wójcik *et al.*, Phys. Rev. A **85**, 012329 (2012).
[41] E. Segawa, J. Comput. Theor. Nanosci. **10**, 1583 (2013).
[42] M. Segev, Y. Silberberg, and D. N. Christodoulides, Nat. Photonics **7**, 197 (2013).
[43] Z. J. Li, J. A. Izaac, and J. B. Wang, Phys. Rev. A **87**, 012314 (2013).
[44] A. Schreiber, K. N. Cassemiro, V. Potoček, A. Gábris, I. Jex, and Ch. Silberhorn, Phys. Rev. Lett. **106**, 180403 (2011).
[45] A. Wójcik, T. Łuczak, P. Kurzyński, A. Grudka, T. Gdala, and M. Bednarska-Bzdega, Phys. Rev. A **85**, 012329 (2012).